

Where i and j are nearest neighbors and $c_{i\sigma}^\dagger$ ($c_{j\sigma}$) is the creation (annihilation) operator of fermions with spin σ , while the hopping elements t_{ij} between the two carbon atoms are randomly obtained. Basic statistic which distinguishes the spectra of integrable systems from chaotic ones is the level-spacing distribution $P^{(k)}(S)$ which $P^{(k)}(S)dS$ represents the probability. The quantity $\langle \rho(E) \rangle (E_{i+k} - E_i)/k$ is located in the interval $(S; S + dS)$, where $E_{i+k} - E_i$ is the distance between k -th neighbors in the level sequence $E_1 \leq E_2 \leq \dots$, and $\langle \rho(E) \rangle$ is the average density of levels in the energy interval $(E, E + dE)$. Due to a quasi-random character of the Hamiltonian, statistical properties of energy levels of large quantum systems are defined by

$$P_{WD,\beta} = \begin{cases} \frac{\pi}{2} S \exp\left(-\frac{\pi S^2}{4}\right) & \beta = 1 & (GOE) \\ \frac{32}{\pi^2} S^2 \exp\left(-\frac{4S^2}{\pi}\right) & \beta = 2 & (GUE) \\ \frac{2^{18}}{3^6 \pi^3} S^4 \exp\left(-\frac{64S^2}{9\pi}\right) & \beta = 4 & (GSE) \end{cases} \quad (3)$$

Also, $P_{Poi}(S) \cong 1 - S$ for $S \rightarrow 0$ and is maximal for $S = 0$, i.e., integrable systems exhibit level attraction which $P_{GOE}(S) \propto S$ for $S \rightarrow 0$ showing linear level repulsion and $P_{GUE}(S) \propto S^2$ for $S \rightarrow 0$ showing stronger (quadratic) level repulsion than GOE. We consider real and symmetric Hamiltonian matrices H in a Hilbert space of dimension N for the GOE which the matrix elements obey $H_{\mu\nu} = H_{\nu\mu} = H_{\mu\nu}^*$ with $\mu, \nu = 1, \dots, N$. In realistic systems Hilbert space has infinite-dimensional and the limit $N \rightarrow \infty$ considered in the sequel which the ensemble described in terms of an integration over matrix elements.

$$\mathcal{P}_\alpha(H)d[H] = \tilde{N}_0 \prod_\mu \exp\left\{-\frac{N}{4\lambda^2} H_{\mu\mu}^2\right\} dH_{\mu\mu} \times \prod_{\rho < \sigma} \exp\left\{-\frac{N}{2\alpha\lambda^2} H_{\rho\sigma}^2\right\} dH_{\rho\sigma} \quad (4)$$

where N_0 is a normalization factor, λ a parameter which defines the average level density and the positive parameter α ranges from zero to one. In applications of the GOE to data, λ is obtained via the empirical average level density. The spectral fluctuation properties of the GOE are then predicted in a parameter-free fashion. In $\alpha = 0$ all non-diagonal elements vanish, and the ensemble consists of diagonal matrices with independent, Gaussian-distributed diagonal elements.

$$\phi_j(x) = (2^j j! \sqrt{\pi})^{-\frac{1}{2}} \exp\left(-\frac{x^2}{2}\right) H_j(x) \quad (5)$$

RMT [23] which generic integrable systems are defined by the Poisson distribution as

$$P^{(k)}(S) = \frac{k^k}{(k-1)!} S^{k-1} \exp(-kS) \quad (2)$$

with $k = 1, 2, \dots$ which the nearest-neighbor spacing distribution $P^{(1)}(S) \equiv P_{Poi}(S) = \exp(-kS)$. In contrast, nearest-neighbor level spacings $P^{(1)}(S)$ of classically chaotic systems which preserve (or break) time-reversal symmetry may be approximated by the so-called Wigner surmise for Gaussian orthogonal ensemble and Gaussian symplectic ensemble (or Gaussian unitary ensemble) of random matrices

The volume element in matrix space $d[H] = \prod_{\mu \leq \nu} dH_{\mu\nu}$ is the product of the differentials $dH_{\mu\nu}$ of the independent matrix elements. In the GOE every state in Hilbert space is connected to itself and to every other state by a matrix element of H which all non-diagonal matrix elements possess the same first and second moments, every state is coupled to all other states with equal average strength. However, this results in level repulsion between any pair of levels, and in a complete mixing of states in Hilbert space. The importance of such coupling existed when we consider a more general ensemble with probability density

The shape of the average spectrum is Gaussian, there is no level repulsion, and the spectral fluctuations are Poissonian. The ensemble coincides with the GOE for $\alpha = 1$ and the shape of the spectrum and the spectral fluctuations interpolate between those two limiting cases for values of α between these two limits. In the GUE, the eigenvalue density obtained by Wigner in 1962 as $\sum_{j=0}^{n-1} \phi_j^2(x)$, where

And $H_j(x)$ is the j th Hermite polynomial, which is defined as:

$$H_j(x) = \exp(x^2) \left(-\frac{d}{dx}\right)^j \exp(-x^2) = j! \sum_{i=0}^{j/2} (-1)^i \frac{(2x)^{j-2i}}{i!(j-2i)!} \quad (6)$$

The following equation considers:

$$\sum_{j=0}^{n-1} \tilde{\phi}_j^2(x) = n\tilde{\phi}_n^2(x) - \sqrt{n(n+1)}\tilde{\phi}_{n-1}(x)\tilde{\phi}_{n+1}(x) \quad (7)$$

Where $\tilde{\phi}_j(x) = (2^j j!)^{-\frac{1}{2}} H_j(x)$. This formula obtained from the famous Christoffel-Darboux relationship for orthogonal polynomials. The probability density for the Tracy-Widom distribution is written as:

$$P(x) = \frac{d}{dx} \exp\left(-\int_x^\infty (t-x)q(t)^2 dt\right) \quad (8)$$

Where $q(t)$ is the solution of a so-called Painleve II differential equation as $\ddot{q}(t) = tq(t) + 2q(t)^3$, with the boundary condition that as $t \rightarrow \infty$, $q(t)$ is asymptotic to the Airy function.

3. Theoretical results

The system of two coupled carbon nanotube oscillators examined in Ref. [24] is an example of the configuration of nanoparticles, which can be a chaotic behaviour which irregular behaviour of many physical systems are the subject of intense experimental and theoretical investigations [25, 26]. Chaotic manifestations can be in systems with different size scales, from the quantum domain [27–29] to stellar dimensions with, for instance, the motion of a relativistic three-body self-gravitating system [30]. The researchers suggested configurations of MWNT nano-oscillators composed of three tubes where the outer one is fixed and both core and inner tube can move. Through rigid body dynamics simulations, they reported typical signatures of soft deterministic chaos, where chaotic and regular regions co-exist. This is the first indication of chaos in nanoscale mechanical systems based on multiwalled carbon nanotube oscillators [31]. Regardless of the presence of chaotic areas, the existence of regular circuits can allow the development of multi-purpose nano devices. Each type can have a particular role in a field of nanomachinery, so the operational blocks for nano-mechanical systems are the proposed scheme by Kang and Hwang [32]. However, the effects of temperature and energy degradation should be carefully considered, as it can lead to undesirable behaviors of the device. Recently, Andreev billiards have risen much experimental [33] and theoretical [34] interest which they are [organized](#) via bringing a ballistic, normal-conducting quantum dot in contact with a superconductor. A characteristic quantity in an Andreev

billiard is the state counting function. However, we point out that the real low-density regime in graphene is dominated entirely by disorder in currently available samples, and therefore a homogeneous carrier density of $n \leq 10^{10} \text{cm}^{-2}$ (10^9cm^{-2}) is unlikely to be accessible for gated samples in the near future. Other calculations within the semi-classical Boltzmann approach or the Landauer approach investigated the effect of screened Coulomb potentials on charge conductivity [35] with similar conclusions, and although the existence of a true universal minimum conductivity could not be rigorously answered, an interpretation in terms of saturation of the conductivity due to charged impurity induced inhomogeneities, occurring at low densities, was reported [36]. Besides the GOE there exist two more canonical random-matrix ensembles: The Gaussian unitary ensemble and the Gaussian symplectic ensemble which the GUE is the Gaussian ensemble of Hermitian (but not necessarily real) matrices and this ensemble plays a role for systems which are not time-reversal invariant. If that invariance does not hold, the Hamiltonian matrix is Hermitian but cannot in general be chosen real and symmetric. In nuclear physics, the GUE is used for tests of time-reversal invariance which is also used as a theoretical testing ground because the calculation of ensemble averages over observables is typically simpler for the GUE than for the GOE. The GSE is used to systems with half-integer spin which are invariant under time reversal, but which are not rotationally invariant and the GSE does not use to nuclei directly. Some of these ensembles have a role in the low-energy behavior of quantum field theories and find application in lattice QCD, the discretized form of quantum chromodynamics which others relate to the scattering of electrons off the interphase between a normal conductor and a superconductor. In the case of (12,0) @ (18,0) DWNT, same results can be drawn with stronger evidences due to the small interlayer distance

which increases the effects. Recently some in-situ transmission electron microscope observations showed this sequential nucleation processes in case of DWNTs by using crystalline Pt as catalyst particle [37].

We calculated the random eigenvalues of the GOE and GUE and obtained the level density of the GUE using Christoffel-Darboux and the tridiagonal matrix for

the double-walled carbon nanotubes in Figure 2 which in the tridiagonal matrix compared for different values of n . Also, we performed Quarter circle Law the double-walled carbon nanotubes which the results are shown for $r=1, 0.1$ in Figure 3.

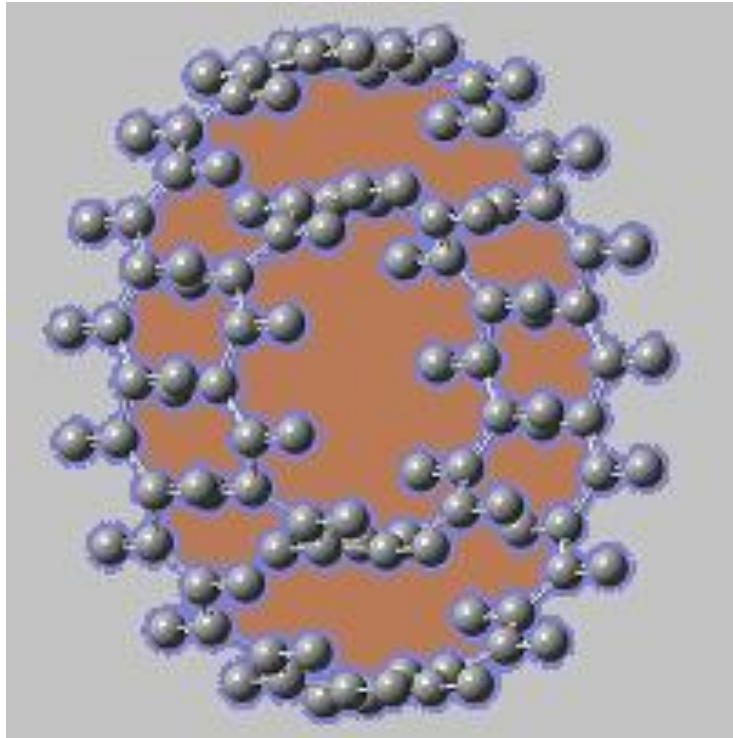


Figure 1. A (10,0) @ (18,0) double-walled carbon nanotubes

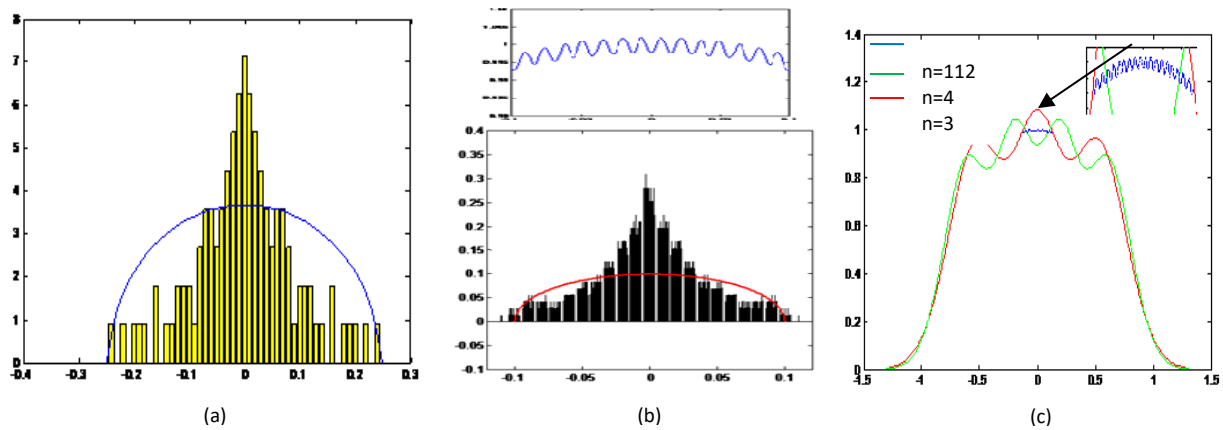


Figure 2. (a) Semicircle Law (Random symmetric matrix eigenvalues) (GOE), (b) calculating the level density for the GUE (in the chart top) and using Christoffel-Darboux (in the chart below), (c) calculating of the level density (GUE) using the tridiagonal matrix for the (10,0) @ (18,0) double-walled carbon nanotubes

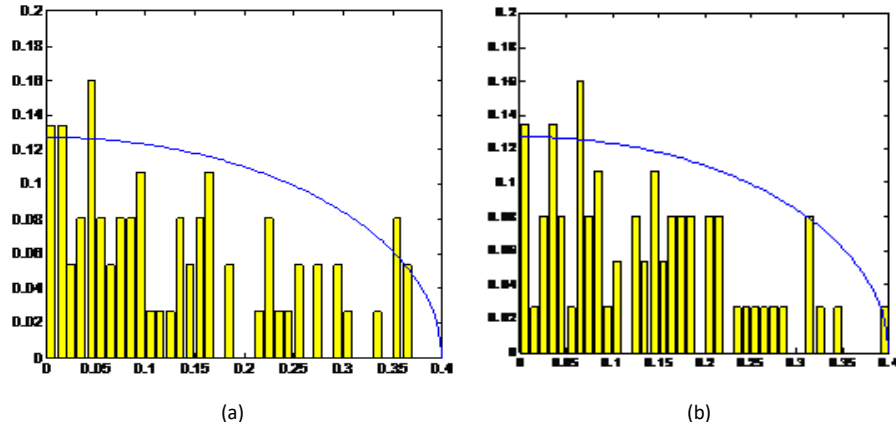


Figure 3. Quarter circle law for (a) $r=1$, (b) $r=0.1$ in the $(10,0) @ (18,0)$ double-walled carbon nanotubes.

One-dimensional quantum dots are currently existed [38, 39], in the form of single-wall carbon nanotubes. The sole orbital symmetry is a two-fold one in nanotubes, corresponding to the $K-K'$ sub band degeneracy and resulting from the equivalence of the two atoms in the primitive cell of the graphene structure which the absence of shell filling in most isolated nanotube dots results from disorder or nonuniformity. Nevertheless, it is expected that the electron system in a nanotube will show the strong

correlation defined by the Luthenger fluid theory, with increasing evidence [40]. Many interesting questions relate to how the correlations relate to the excitation spectrum, the disorder, and the small exchange terms that allow spin shells to be shown. The Tracy-Widom Distribution, largest eigenvalues of a random Hermitian matrix and the angles of its eigenvalues of the random unitary matrix which distributed on the unit circle in the complex plane in the double-walled carbon nanotubes are shown in Figure 4

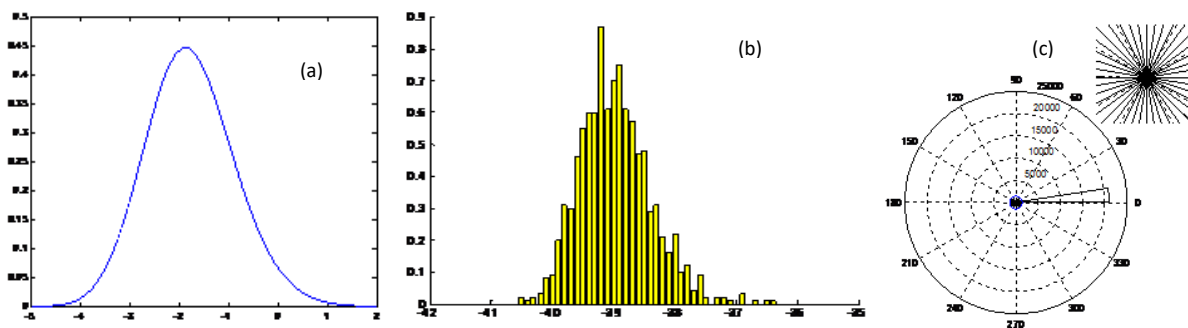


Figure 4. (a) Calculating the Tracy-Widom Distribution, (b) Largest Eigenvalues of a random Hermitian matrix with trial =1000 and (c) histograms the angles of its eigenvalues of the random unitary matrix in the $(10,0) @ (18,0)$ double-walled carbon nanotubes

Investigating chaotic properties in a finite double-walled carbon nanotube is important because its geometric and its electronic properties which translation invariance holds in both directions. But an infinite system is ideal, and sooner or later it is a task to analyze the electronic properties of finite or semi-infinite systems, and especially the system with boundaries. For example, it's important that carbon nanotube is important in an electrical circuit or any other device. It is important that

the electronic properties differ between an infinite double-walled carbon nanotube and a system with boundaries such as the nanoribbons. In particular, the presence of boundaries may completely alter the spectrum and structure of Dirac's points. The energy dispersion and chaos are known to be strongly related to the geometry of the boundaries [41]. When increasing the power of the disorder, the transfer from Poisson to the GUE distribution occurs. For a constant power

disorder in the chaos range and increasing the number of gaps in the edge, we see the transition to the GOE the evolution of the GUE distribution with dual degradation showed to the specific distribution of two independent GUEs in a weak magnetic field.

4. Conclusions

We have studied symmetric and asymmetric classes of nano systems selected in the (10,0) @ (18,0) double-walled carbon nanotubes and examined the quantum chaos in these systems using random matrix matrices. In the absence of disturbances and chaos, the analytical solutions available for Dirac's continuous billiard show that surface clustering is due to number-theoretic degeneracies. Because of nonlinearity, such degenerations exist in the tight coupling model. The conditions in the dispersion relation lead to the distribution of the poison of the energy level which characteristic for the integrable system. For weak disorders, transition to quantum chaos is seen. In such a limited range, spectral statistics follow these Gaussian ensembles of random matrices. In principle, all the tight-binding Hamiltonians are time-reversal invariant and it is expected that in the absence of a magnetic field, the symmetry class will be orthogonal. The Tracy-Widom Distribution and largest eigenvalues of a random Hermitian matrix are calculated. Indeed, the main hurdle in the development of a DWNT based technology considered to control their structure and more precisely their diameter and chirality.

5. References

[1] Ullmo, D., (2007). Rep. Prog. Phys. arXiv:0712.1154v1 [cond-mat.mes-hall] 7 Dec.

[2] Dresselhaus, M. S., Dresselhaus, G., Eklund P.C., (1996). Science of Fullerenes and Carbon Nanotubes (Academic Press, New York 1996); R. Saito, G. Dresselhaus, M.S. Dresselhaus: Physical Properties of Carbon Nanotubes, Imperial College Press, London.

[3] Kim, P., et al., (2001). Thermal transport measurements of individual multiwalled nanotubes. Physical Review Letters, 87 (21): p. 2155021-2155024.

[4] J.O'Connell, M., ed., (2015). Carbon Nanotubes: Properties and Applications. 2006 Taylor and Francis: United States of America; Koshino, M., Moon, P., and Son, Y. W., Phys. Rev. B 91, 035405.

[5] Sinnott, S. B., and Andrews, R., (2001). Crit. Rev. Solid State Material Science. 26 145.

[6] Rinzler, A. G., Hafner, J. H., Nikolaev, P., Lou, L., Kim, S. G., Tomanek, D., Nordland, R. P., Colbert, D. T., and Smalley, R. E., (1995). Science. 269 1550.

[7] Tans, S. J., Devoret, M. H., Dal, H., Thess, A., Smalley, R. E., Geerligs, L. J., and Dekker, C., (1997). Nature, 386 474.

[8] Cumings, J., Zettl, A., (2000). Science, 289 602.

[9] Zheng, Q., Jiang, Q., (2002). Phys. Rev. Lett, 88 045503.

[10] Zheng, Q., Liu, J. Z., and Jiang, Q., (2002). Phys. Rev. B, 65 245409.

[11] Legoas S B, Coluci V R, Braga S F, Coura P Z, Dantas S O and Galvˆao D S 2003 Phys. Rev. Lett. 90 055504.

[12] Legoas S. B., Coluci V. R., Braga S. F., Coura P. Z., Dantas S. O., and Galvˆao D. S., (2004). Nanotechnology, 15 S184.

[13] Guo W., Guo Y., Gao H., Zheng Q., and Zhong W., (2003). Phys. Rev. Lett. 91 125501.

[14] Zhao Y, Ma C-C, Chen G and Jiang Q (2003). Phys. Rev. Lett. 91 175504.

[15] Rivera J. L., McCabe C., and Cummings P. T., (2003). Nano Lett. 3 1001.

[16] Rivera J. L., McCabe C., and Cummings P. T., (2005). Nanotechnology 16 186.

[17] Tangney P, Louie S G and Cohen M L 2004 Phys. Rev. Lett. 93 065503.

[18] Kang J. W., and Hwang H. J., (2004). Appl. Phys. 96 3900.

[19] Berry M.V., and Mondragon, R.J., (1987). Proc. R. Soc. A 412, 53.

[20] Ponomarenko, L.A., Schedin, F., Katsnelson, M.I., Yang, R., Hill, E.W., Novoselov, K.S., and Geim, A.K., (2008). Science, 320, 356.

[21] E. Abrahams, P. W. Anderson, D. C. Licciardello, and T. Ramakrishnan, Phys. Rev. Lett. 42 (1979) 673.

[22] Mello, P. A., and Kumar, N., (2004). Quantum Transport in Mesoscopic Systems, (Oxford University Press, Oxford.

[23] M.L. Mehta, (2004)., Random Matrices, 3rd ed., Elsevier, Amsterdam.

[24] Coluci, V. R., Legoas, S. B., Mde Aguiar M. A., and Galvao, D. S., (2005). Nanotechnology 16 583–589.

[25] Ott, E., (1993). Chaos in Dynamical Systems, Cambridge University Press.

[26] Gutzwiller, M C., (1990). Chaos in Classical and Quantum Mechanics, Springer, New York.

[27] Jensen, R. V., (1982). Phys. Rev. Lett. 49 1365.

[28] Jensen, R. V., (1984). Phys. Rev. A 30 386.

- [29] Jensen, R. V., (1987). *Phys. Scr.* 35 668.
- [30] Burnell, F., Mann, R. B., and Ohta, T., (2003). *Phys. Rev. Lett.* 90 134101.
- [31] Zheng, Q., and Jiang, Q., (2002). *Phys. Rev. Lett.* 88 045503.
- [32] Kang, J. W., Hwang, H. J., (2004). *Nanotechnology*, 15 1633.
- [33] Morpurgo, A. F., Holl, S., van Wees, B. J., Klapwijk, T. M., and Borghs, G., (1997). *Phys. Rev. Lett.* 78:2636.
- [34] Lambert, C. J., and Raimondi, J. R., (1998). *Phys. Condens. Matter*, 10:901.
- [35] Khveshchenko, D. V., (2007). *Phys. Rev. B*, 75, 241406.
- [36] Dong, H. M., Xu, W., Zeng, Z., Peters, F. M., (2008). *Phys. Rev. B*, 77, 235402.
- [37] Zhang, L., Kling, K., and Wagner, J., (2016). Private communications.
- [38] Tans, S., et al., (1997). *Nature*, 386, 474.
- [39] Bockrath M., et al., (1997). *Science*, 275, 229.
- [40] Bockrath M., et al., (1999). *Nature*, 397, 598.
- [41] Cresti, A., Nemeč, N., Biel, B., Niebler, G., Triozon, F., Cuniberti, G., and Roche, S., (2008). *Nano Res. fig.* 1:361.